RSC Advances

ROYAL SOCIETY OF CHEMISTRY

www.rsc.org/advances

Cite this: DOI: 10.1039/c0xx00000x

www.rsc.org/xxxxxx

Communication

Effects of electrolytes on the capacitive behaviors of nitrogen/phosphorus co-doped nonporous carbon nanofibers: Insight into the role of phosphorus groups

Xiaodong Yan, Yunhua Yu,* and Xiaoping Yang

Received (in XXX, XXX) XthXXXXXXXXX 20XX, Accepted Xth XXXXXXXXX 20XX
DOI: 10.1039/b000000x

The emerging need for high-power energy storage/release systems has promoted the development of supercapacitors, which can provide higher power density as well as much longer cycle life as compared to batteries.[1,2] Carbon materials have been the most widely studied electrode materials for supercapacitors because of their structural versatility, such as activated carbons, carbon nanofibers, carbon nanotubes, and graphene.[3,4] Although tremendous efforts have been made to develop high-performance carbon electrodes, the energy density for carbon-based electrodes is still orders of magnitude lower than batteries. Therefore, extensive and intensive researches have been devoted to increasing the specific capacitance of carbon materials by introducing metal oxides,[5] conducting polymers[6] and/or functional groups (such as nitrogen and phosphorus groups)[7,8] into carbon materials. Transitional metal oxides and conducting polymers can provide much larger pseudocapacitance than that of functional groups. Nevertheless, these materials experience fast capacitance degradation during the charge/discharge processes, limiting their practical applications. Heteroatom functionalization of carbon materials will not deteriorate the cyclability, making it a practical way to develop high-capacitance carbon electrodes for commercial use.

Nitrogen and phosphorus co-doped carbons have recently attracted much attention due to their outstanding electrochemical performance.[9-13] For instance, Nasini et al. reported the preparation of nitrogen/phosphorus co-doped mesoporous carbon which presented small surface area of 479 m^2 g^{-1} but very high capacitance (271 F g^{-1} in 1 M H_2SO_4 and 236 F g^{-1} in 6 M KOH).[13] Nitrogen groups have been proved to be electrochemically active groups which can offer high pseudocapacitance through reversible redox reactions.[14,15] However, the role of phosphorus groups is not known exactly. Therefore, it makes great sense to identify the true role of phosphorus groups in carbon-based electrodes for future optimal design and fabrication of high-performance nitrogen/phosphorus co-doped carbon materials. Often, the co-existence of micropores and heteroatom groups makes it complex to study the true role of the heteroatom groups. Since we recently have synthesized the nitrogen/phosphorus co-doped nonporous carbon nanofibers by electrospinning of precursor solution containing polyacrylonitrile (PAN) and phosphoric acid and subsequent thermal treatments,[12] the impact of the porosity on the capacitance can be avoided, making it possible to identify the role of phosphorus groups definitely. Hence, the present work investigates the capacitive behaviors of such nitrogen/phosphorus co-doped nonporous carbon nanofibers (N/P-NPCNFs) in different electrolytes (e.g. 1 M H_2SO_4, 0.5 M Li_2SO_4, 1 M Na_2SO_4 and 0.5 M K_2SO_4). Also, the capacitive behaviors of pure nitrogen-doped nonporous carbon nanofibers (N-NPCNFs) derived from PAN were studied in these electrolytes. New insight into the role of phosphorus groups in enhancing the electric double layer (EDL) capacitance of carbon materials was provided.

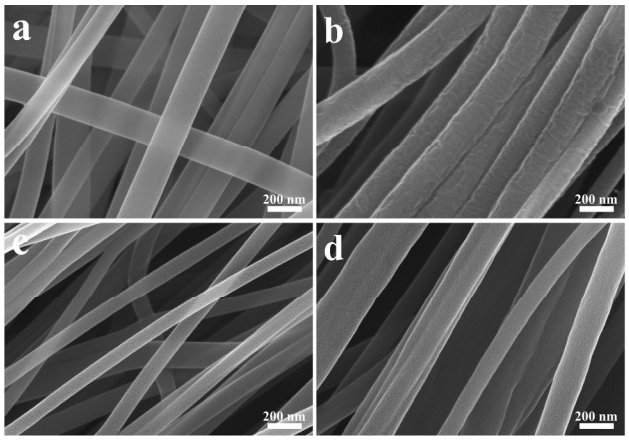

Fig. 1 SEM images of (a) pure PAN nanofibers, (b) H_3PO_4/PAN composite nanofibers, (c) nitrogen-doped carbon nanofibers, and (d) nitrogen/phosphorus co-doped carbon nanofibers.

Fig. 1 shows the typical SEM images of the precursor nanofibers and carbon nanofibers. All the nanofibers demonstrate long, continuous fibrous morphologies. Obviously, the introduction of phosphoric acid greatly changed the physical properties of the precursor solution, leading to different surface morphologies and diameters for the precursor nanofibers (Fig. 1a and b). That is, pure PAN nanofibers possess very smooth surface while the H_3PO_4/PAN composite nanofibers present rough surface as well as a larger average diameter. After carbonization, the surface morphologies of N/P-NPCNFs and N-NPCNFs are both smooth (Fig. 1c and d), and the average diameter of N/P-

NPCNFs is still much larger than that of N-NPCNFs.

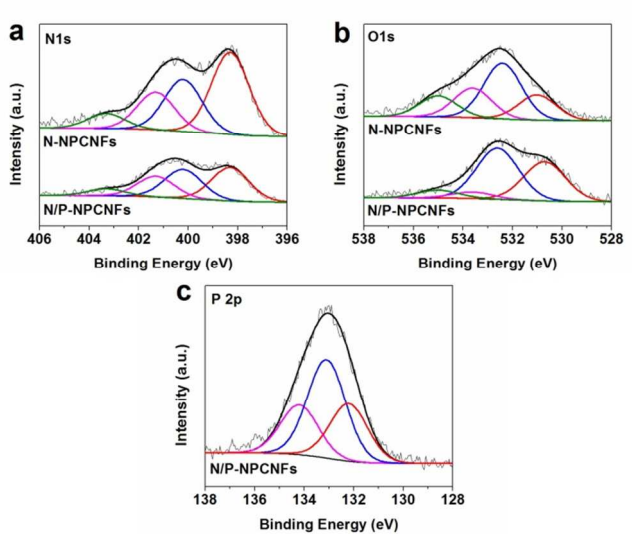

Fig. 2 XPS spectra of N-NPCNFs and N/P-NPCNFs.

As proposed elsewhere,[12] the N1s spectrum (Fig. 2a) can be deconvoluted into four different components: the peaks at 398.3, 400.4, 401.1 and 403.3 eV are ascribed to pyridinic nitrogen and P=N bond, pyridonic/pyrrolic nitrogen (pyrrol-like nitrogen), quaternary nitrogen and P-N bond, pyridine-N-oxide, respectively.[16,17] It is clearly that the content of the pyrrol-like nitrogen in N/P-NPCNFs is much greater than that in N-NPCNFs according to the XPS spectra. The O1s spectrum can be divided into five regions (Fig. 2b), which represent C=O including quinones and non-bridging oxygen in the phosphate groups (P=O) (531.0 eV); oxygen single bonded to carbon in C-O and in C-O-P groups (532.6 eV); oxygen single bonds in hydroxyl groups (533.6 eV) and carboxylic groups (–COOH) and/or water (535.0 eV).[18,19] The fine structure of P2p peak (Fig. 2c) points to the presence of three major phosphorus groups differentiated by their binding energies: C-O-P groups (134.2 eV); C-PO_3 or C_2-PO_2 groups (133.1 eV); C_3-P groups (132.2 eV).[18] More details about the XPS analyses can be found in Ref 12.

Fig. 3 shows the cyclic voltammograms of N-NPCNFs in different electrolytes at the scan rate of 10 mV s^{-1}. The cyclic voltammogram of the N-NPCNFs electrode is more close to a triangular shape in 1 M H_2SO_4 (Fig. 3a), indicating poor EDL behavior. However, the N-NPCNFs electrode still exhibits relatively high capacitance due to the pseudocapacitive interactions between the H^+ ions and heteroatom (nitrogen and oxygen) groups. Previous research showed that nitrogen-doped carbons store energy by simple electrostatic interaction between electrolyte ions and charge at the electrode surface in neutral electrolytes.[20] Thus, very poor capacitive behaviors for the N-NPCNFs electrode in 0.5 M Li_2SO_4 (Fig. 3b), 1 M Na_2SO_4 (Fig. 3c) and 0.5 M K_2SO_4 (Fig. 3d) were observed, showing tremendously distorted rectangular shapes and extremely small capacitance and thus confirming the nonporous characteristics of N-NPCNFs.

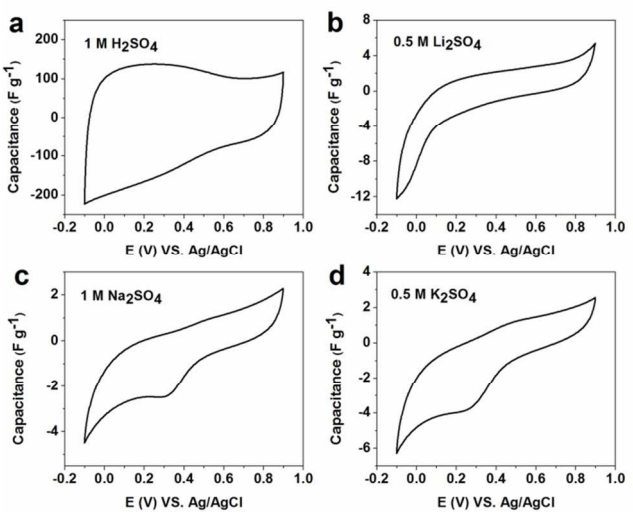

Fig. 3 Cyclic voltammograms of N-NPCNFs obtained in different electrolytes at 10 mV s^{-1}.

Fig. 4 shows the cyclic voltammograms of N/P-NPCNFs in different electrolytes at the scan rate of 10 mV s^{-1}. It is worth noting that although the specific surface area of N/P-NPCNFs is much smaller than that of N-NPCNFs (see Ref 12), the N/P-NPCNFs electrodes present greatly improved capacitive properties in all electrolytes due to the introduction of phosphorus groups. The cyclic voltammogram of the N/P-NPCNFs electrode is a nearly-rectangular shape in 1 M H_2SO_4 (Fig. 4a), indicating that the phosphorus groups mainly enhances the EDL capacitance. Obviously, no difference in the redox humps for N-NPCNFs and N/P-NPCNFs is observed in H_2SO_4 electrolyte, implying that phosphorus groups are not electrochemically active. In the neutral electrolytes, the N/P-NPCNFs electrode shows the best capacitive behavior in 0.5 M K_2SO_4 with the cyclic voltammogram of a slightly distorted rectangular shape (Fig. 4d). Though the cyclic voltammogram of the N/P-NPCNFs electrode in 0.5 M Li_2SO_4 is far from a rectangular shape (Fig. 4b), it is much better than that of the N-NPCNFs electrode in 0.5 M Li_2SO_4. As is expressed by the cyclic voltammogram in Fig. 4c, the capacitive behavior of the N/P-NPCNFs electrode in 1 M Na_2SO_4 falls in between those in 0.5 M Li_2SO_4 and 0.5 M K_2SO_4. These results suggest that phosphorus-functionalized carbon surface is very attractive to electrolyte ions due to the presence of oxygen-rich phosphorus groups.

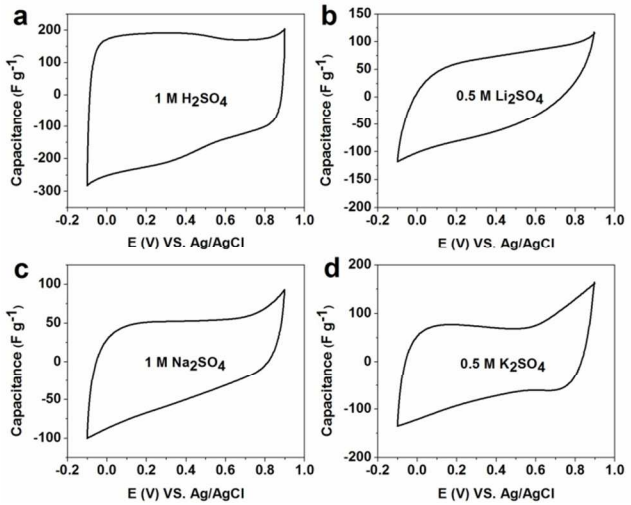

Fig. 4 Cyclic voltammograms of N/P-NPCNFs obtained in different electrolytes at 10 mV s^{-1}.

It is considered that the galvanostatic charge/discharge measurement is a more accurate technique to estimate the capacitance, especially the pseudocapacitance. Therefore, specific capacitances of N-NPCNFs and N/P-NPCNFs in different electrolytes as a function of current density are plotted in Fig. 5a and b, respectively. The specific capacitance in the present case was calculated from the galvanostatic charge/discharge profiles based on the following equation:

$$C = i\Delta t/m\Delta V \quad (1)$$

where C (F g^{-1}) is the specific capacitance, i (A) refers to the discharge current, ΔV (V) represents the potential window within the discharge time Δt (s), and m (g) corresponds to the amount of active material on the electrode.[21] In order to roughly estimate the EDL capacitance originated from phosphorus groups, we speculate that the total capacitance is the sum of the capacitances that come from the nitrogen, oxygen and phosphorus groups. Therefore, the capacitance provided by phosphorus groups can be roughly obtained by the following equation:

$$C_p = C_{N/P} - C_N \quad (2)$$

where C_p (F g^{-1}) is the capacitance induced by phosphorus groups, and $C_{N/P}$ (F g^{-1}) and C_N (F g^{-1}) represent the specific capacitances of the N/P-NPCNFs electrode and the N-NPCNFs electrode, respectively. The capacitance values calculated according to equation (1) and (2) are listed in Table 1. Obviously, the capacitance of the N-NPCNFs electrode in neutral electrolytes is negligible, while the capacitance of the N/P-NPCNFs electrode increased greatly in those neutral electrolytes as well as in the acidic electrolyte. These results agree well with the results of the CV measurements. The capacitance derived from phosphorus groups in different electrolytes increases in the order of H_2SO_4 > K_2SO_4 ≈ Li_2SO_4 > Na_2SO_4. In general, the difference in capacitance as well as in rate capability may be related to (I) the crystal radius of the ions, (II) the radius of the ionic hydration sphere in aqueous solution, (III) the conductivity of the electrolyte, (IV) the mobility of the ions, and (V) the solvation/desolvation energy for the ions in aqueous electrolytes. It is well known that H^+ ions and alkali metal ions are strongly solvated in aqueous solution with the increase of the ion-solvent complex diameter in the order of $Li^+ > Na^+ > K^+ > H^+$, and the crystal radius of the ions decreases in the sequence of $K^+ > Na^+ > Li^+ > H^+$.[22-24] It seems that the EDL capacitance provided by the phosphorus groups is more related to the crystal radius of the electrolyte ions. This suggests that the adsorbed electrolyte ions by the phosphorus groups might partially desolvate, shortening the distance between the carbon surface and the adsorbed ions, which may explain the tremendously high EDL capacitance per unit area (~ 8.5 F m^{-2} in acidic electrolyte) that only originated from the phosphorus groups. It should be noted that the larger capacitance in 0.5 M K_2SO_4 compared with that in 1 M Na_2SO_4 could be attributed to the high content of pyrrol-like nitrogen groups in N/P-NPCNFs (accounting for 65.4% of the total nitrogen groups[12]), which are proved to have strong binding to the K^+ ions.[15] It can be further verified by the similar capacitance for the N/P-NPCNFs electrode in 1 M Na_2SO_4 and 0.5 M K_2SO_4 at the high current density of 5 A g^{-1}, because the advantage of the strong adsorption of K^+ to pyrrol-like nitrogen configurations may diminish under the condition of fast ion transport. Thus, nitrogen groups contribute a lot to the total capacitance of N/P-NPCNFs in K_2SO_4 electrolyte at low current densities.

Table 1 Specific capacitance (F g^{-1}) of the samples in each electrolyte at 0.5 A g^{-1} and the roughly estimated capacitance (F g^{-1}) from phosphorus groups

	1 M H_2SO_4	0.5 M Li_2SO_4	1 M Na_2SO_4	0.5 M K_2SO_4
N-NPCNFs	121	2.4	1.5	1.5
N/P-NPCNFs	223	78	53	82
C_P	102	75.6	51.5	80.5

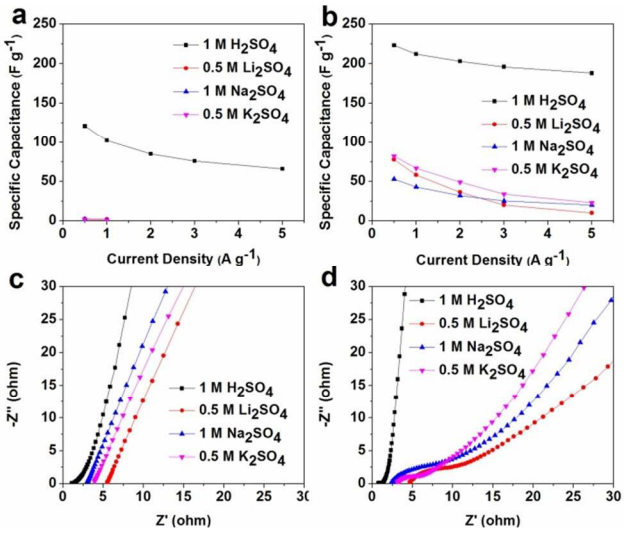

Fig. 5 Specific capacitance as a function of current density for (a) N-NPCNFs and (b) N/P-NPCNFs in different electrolytes; Nyquist plots of (c) N-NPCNFs and (d) N/P-NPCNFs in different electrolytes.

In order to clearly evaluate the effects of electrolyte ions on the capacitive properties, EIS measurement is performed and the Nyquist plots are shown in Fig. 5c and d. The linear part in the Nyquist plot in the high-frequency region is related to the ion diffusion process; the semicircle in the medium-frequency region

is a measure of the interfacial charge transfer resistance (R_{ct}); and the intercept value of the curve with the real axis in the high-frequency region represents the equivalent series resistance (R_{ERS}).[15,25] For the N-NPCNFs electrode (Fig. 5c), the linear part of the Nyquist plot obtained in 1 M H_2SO_4 exhibits the largest slop value, indicating fast formation rate of EDL[15] maybe due to the alkaline properties of the nitrogen groups (facilitating the adsorption of H^+ ions). Furthermore, the semicircle confirms the presence of redox reactions between heteroatom (mainly nitrogen) groups and H^+ ions, and the small diameter of the semicircle suggests a small R_{ct}. Obviously, the R_{ERS} varies according to the electrolyte, increasing in the sequence of Li_2SO_4 > K_2SO_4 > Na_2SO_4 > H_2SO_4. The R_{ERS} of the N/P-NPCNFs electrode in different electrolytes has the same trend (Fig. 5d). These results indicate that the conductivity of the electrolyte, in the present case, increases in the order: 1 M H_2SO_4 > 1 M Na_2SO_4 > 0.5 M K_2SO_4 > 0.5 M Li_2SO_4. However, the R_{ERS} of the N/P-NPCNFs electrode is always smaller than that of the N-NPCNFs electrode in every electrolyte, suggesting a decrease of the contact resistance between the electrode and the electrolyte due to the greatly enhanced surface wettability of the carbon nanofibers induced by the phosphorus groups. Furthermore, the nearly-vertical line in the Nyquist plot of the N/P-NPCNFs electrode obtained in 1 M H_2SO_4 shows much better capacitive behavior as compared to that of the N-NPCNFs electrode, confirming that the introduction of phosphorus groups really facilitate the adsorption of H^+ ions. It is further confirmed by the smaller R_{ct} (0.27 Ω) as compared with that (0.48 Ω) of the N-NPCNFs electrode in 1 M H_2SO_4.

Interestingly, relatively large semicircles were observed in the Nyquist plots of the N/P-NPCNFs electrodes in neutral electrolytes, whereas no semicircles were observed in the Nyquist plots of the N-NPCNFs electrodes in neutral electrolytes. This could be attributed to the enhanced adsorption of the electrolyte ions onto the surface of the nonporous carbon nanofibers, leading to greatly increased charge transfer and thus enhanced redox reactions. Apparently, in neutral electrolytes, the N/P-NPCNFs electrode in 0.5 M K_2SO_4 presents the smallest R_{ct}, confirming the strong binding between K^+ ions and pyrrol-like nitrogen groups and thus giving rise to relatively fast charge transfer. Furthermore, the slop value of the line in the Nyquist plot for the N/P-NPCNFs electrode in 0.5 M Li_2SO_4 is the smallest, suggesting a very slow ion diffusion process. Therefore, it can be concluded that the smallest electrolyte conductivity and the low diffusion coefficient of Li^+ ions lead to the worst rate performance of the N/P-NPCNFs electrode in 0.5 M Li_2SO_4 (12.8% capacitance retention in the current range of 0.5–5 A g^{-1}). In addition, the rate capability is also related to the binding energy between the electrolyte ions and the surface groups. In this case, phosphorus groups have stronger interactions with the H^+ ions due to the hydrogen interactions between H^+ ions and oxygen. The excellent rate capability (84.3% capacitance retention) of the N/P-NPCNFs electrode in 1 M H_2SO_4 may be explained by the following reasons: high electrolyte conductivity, high ionic mobility, and the hydrogen interactions between H^+ ions and oxygen-rich phosphorus groups (which make a great number of H^+ ions locate at the electrode/electrolyte interface and thus shorten the ion diffusion distance from electrolyte to carbon surface).

Conclusions

In summary, cyclic voltammetry, galvanostatic charge/discharge and electrochemical impedance spectroscopy measurements have been employed to comparatively and comprehensively study the electrochemical performances of N/P-NPCNFs and N-NPCNFs in different electrolytes (1 M H_2SO_4, 0.5 M Li_2SO_4, 1 M Na_2SO_4 and 0.5 M K_2SO_4). The electrochemical measurements show that N-NPCNFs demonstrate no capacitive properties in neutral electrolytes, and that phosphorus groups play a crucial role in improving the EDL behavior of the nonporous carbon nanofibers by greatly enhancing the surface wettability of carbon and the ability to adsorb electrolyte ions. Furthermore, the specific capacitance and rate capability of N/P-NPCNFs in different electrolytes are related to the crystal size of the ions, electrolyte conductivity and ionic mobility. In addition, the superior capacitive behavior of N/P-NPCNFs in acidic electrolyte may also be correlated with the hydrogen interactions between H^+ ions and oxygen-rich phosphorus groups.

Acknowledgements

The authors acknowledge the financial supports from National Natural Science Foundation of China (Nos. 51072013, 51272021, 51142004) and Natural Science Foundation of Jiangsu Province (BK20131147).

Notes and References

State Key Laboratory of Organic-inorganic Composite, Beijing University of Chemical Technology, Beijing 100029 (China). Fax: +8610-64412084; Tel: 8610-64412084; E-mail: yuyh@mail.buct.edu.cn

†Electronic Supplementary Information (ESI) available: Detailed experimental procedures. See DOI: 10.1039/b000000x/

1 A. Izadi-Najafabadi, T. Yamada, D. N. Futaba, M. Yudasaka, H. Takagi, H. Hatori, S. Iijima and K. Hata, ACS Nano, 2011, 5, 811.
2 M. G. Hahm, A. L. M. Reddy, D. P. Cole, M. Rivera, J. A. Vento, J. Nam, H. Y. Jung, Y. L. Kim, N. T. Narayanan, D. P. Hashim, C. Galande, Y. J. Jung, M. Bundy, S. Karna, P. M. Ajayan and R. Vajtai, Nano Lett., 2012, 12, 5616.
3 H. Jiang, P. S. Lee and C. Li, Energy Environ. Sci., 2013, 6, 41.
4 S. Bose, T. Kuila, A. K. Mishra, R. Rajasekar, N. H. Kim and J. H. Lee, J. Mater. Chem., 2012, 22, 767.
5 A. Jena, N. Munichandraiah and S. A. Shivashankar, J. Power Sources, 2013, 237, 156.
6 Z. Niu, P. Luan, Q. Shao, H. Dong, J. Li, J. Chen, D. Zhao, L. Cai, W. Zhou, X. Chen and S. Xie, Energy Environ. Sci., 2012, 5, 8726.
7 Y. S. Yun, J. Shim, Y. Tak and H.-J. Jin, RSC Adv., 2012, 2, 4353.
8 D. Hulicova-Jurcakova, A. M. Puziy, O. I. Poddubnaya, F. Suárez-García, J. M. D. Tascón and G. Q. Lu, J. Am. Chem. Soc., 2009, 131, 5026.
9 C.Wang, L. Sun, Y. Zhou, P. Wan, X. Zhang and J. Qiu, Carbon, 2013, 59, 537.
10 C.Wang, Y. Zhou, L. Sun, Q. Zhao, X. Zhang, P. Wan and J. Qiu, J. Phys. Chem. C, 2013, 117, 14912.
11 C.Wang, Y. Zhou, L. Sun, P. Wan, X. Zhang and J. Qiu, J. Power Sources, 2013, 239, 81.
12 X. Yan, Y. Liu, X. Fan, X. Jia, Y. Yu and X. Yang, J. Power Sources, 2014, 248, 745.

13 U. B. Nasini, V. G. Bairi, S. K. Ramasahayam, S. E. Bourdo, T. Viswanathan and A. U. Shaikh, J. Power Sources, 2014, 250, 257.

14 M. Zhong, E. K. Kim, J. P. McGann, S.-E. Chun, J. F. Whitacre, M. Jaroniec, K. Matyjaszewski and T. Kowalewski, J. Am. Chem. Soc., 2012, 134, 14846.

15 F. M. Hassan, V. Chabot, J. Li, B. K. Kim, L. Ricardez-Sandoval and A. Yu, J. Mater. Chem. A, 2013, 1, 2904.

16 W.B. Perry, T.F. Schaaf and W.L. Jolly, J. Am. Chem. Soc., 1975, 97, 4899.

17 J.R. Pels, F. Kapteijn, J.A. Moulijn, Q. Zhu and K.M. Thomas, Carbon, 1995, 33, 1641.

18 A.M. Puziy, O.I. Poddubnaya, R.P. Socha, J. Gurgul and M. Wisniewski, Carbon, 2008, 46, 2113.

19 R. Arrigo, M. Hävecher, S. Wrabetz, R. Blume, M. Lerch, J. McGregor, E.P.J. Parrott, J.A. Zeitler, L.F. Gladden, A. Knop-Gericke, R. Schlögl and D.S. Su, J. Am. Chem. Soc., 2010, 132, 9616.

20 D. Hulicova, J. Yamashita, Y. Soneda, H. Hatori and M. Kodama, Chem. Mater., 2005, 17, 1241.

21 L. Zhao, L.-Z. Fan, M.-Q. Zhou, H. Guan, S. Qiao, M. Antonietti and M.-M. Titirici, Adv. Mater., 2010, 22, 5202.

22 X. Zhang, X. Wang, L. Jiang, H. Wu, C. Wu and J. Su, J. Power Sources, 2012, 216, 290.

23 W. Gu, M. Sevilla, A. Magasinski, A. B. Fuertes and G. Yushin, Energy Environ. Sci., 2013, 6, 2465.

24 K. Fic, G. Lota, M. Meller and E. Frackowiak, Energy Environ. Sci., 2012, 5, 5842.

25 L.-Q. Mai, A. Minhas-Khan, X. Tian, K. M. Hercule, Y.-L. Zhao, X. Lin and X. Xu, Nat. Commun., 2013, 4, 2924.